

Neuropharmacology

Elsevier Editorial System(tm) for

Manuscript Draft

Manuscript Number: NEUROPHARM-D-18-00250R1

Title: Methylene blue activates the PMCA activity and cross-interacts with amyloid β -peptide, blocking $A\beta$ -mediated PMCA inhibition

Article Type: Research Paper

Keywords: Methylene blue; PMCA; $A\beta$; molecular interactions; neuronal Ca^{2+} dysregulation

Corresponding Author: Professor Ana Mata,

Corresponding Author's Institution: Universidad de Extremadura

First Author: Maria Berrocal

Order of Authors: Maria Berrocal; Isaac Corbacho; Carlos Gutierrez-Merino; Ana Mata

Abstract: The phenothiazine methylene blue (MB) is attracting increasing attention because it seems to have beneficial effects in the pathogenesis of Alzheimer's disease (AD). Among other factors, the presence of neuritic plaques of amyloid- β peptide ($A\beta$) aggregates, neurofibrillar tangles of tau and perturbation of cytosolic Ca^{2+} are important players of the disease. It has been proposed that MB decreases the formation of neuritic plaques due to $A\beta$ aggregation. However, the molecular mechanism underlying this effect is far from clear. In this work, we show that MB stimulates the Ca^{2+} -ATPase activity of the plasma membrane Ca^{2+} -ATPase (PMCA) in human tissues from AD-affected brain and age-matched controls and also from pig brain and cell cultures. In addition, MB prevents and even blocks the inhibitory effect of $A\beta$ on PMCA activity. Functional analysis with mutants and fluorescence experiments strongly suggest that MB binds to PMCA, at the C-terminal tail, in a site located close to the last transmembrane helix and also that MB binds to the peptide. Besides, $A\beta$ increases PMCA affinity for MB. These results point out a novel molecular basis of MB action on $A\beta$ and PMCA as mediator of its beneficial effect on AD.

Methylene blue activates the PMCA activity and cross-interacts with amyloid β -peptide, blocking $A\beta$ -mediated PMCA inhibition

Maria Berrocal, Isaac Corbacho, Carlos Gutierrez-Merino, Ana M. Mata*

Departamento de Bioquímica y Biología Molecular y Genética, Facultad de Ciencias, Universidad de Extremadura and Instituto Universitario de Biomarcadores de Patologías Moleculares, Universidad de Extremadura, Badajoz 06006, Spain

E-mail addresses: M.B., mabeca@unex.es; I.C., icorbacho@unex.es; C.G.-M., carlosgm@unex.es; A.M.M., anam@unex.es

*Corresponding author: Ana M. Mata

anam@unex.es

Departamento de Bioquímica y Biología Molecular y Genética, Facultad de Ciencias, Universidad de Extremadura and Instituto de Biomarcadores de Patologías Moleculares", Universidad de Extremadura, Badajoz 06006, Spain

ABSTRACT

The phenothiazine methylene blue (MB) is attracting increasing attention because it seems to have beneficial effects in the pathogenesis of Alzheimer's disease (AD). Among other factors, the presence of neuritic plaques of amyloid- β peptide ($A\beta$) aggregates, neurofibrillar tangles of tau and perturbation of cytosolic Ca^{2+} are important players of the disease. It has been proposed that MB decreases the formation of neuritic plaques due to $A\beta$ aggregation. However, the molecular mechanism underlying this effect is far from clear. In this work, we show that MB stimulates the Ca^{2+} -ATPase activity of the plasma membrane Ca^{2+} -ATPase (PMCA) in human tissues from AD-affected brain and age-matched controls and also from pig brain and cell cultures. In addition, MB prevents and even blocks the inhibitory effect of $A\beta$ on PMCA activity. Functional analysis with mutants and fluorescence experiments strongly suggest that MB binds to PMCA, at the C-terminal tail, in a site located close to the last transmembrane helix and also that MB binds to the peptide. Besides, $A\beta$ increases

PMCA affinity for MB. These results point out a novel molecular basis of MB action on A β and PMCA as mediator of its beneficial effect on AD.

HIGHLIGHTS

Methylene blue activates the PMCA pump

Methylene blue blocks the toxic effect of A β on PMCA

The A β peptide increases MB affinity for PMCA

KEYWORDS: Methylene blue; PMCA; A β ; molecular interactions; neuronal Ca²⁺ dysregulation

ABBREVIATIONS: A β , amyloid β -peptide; AD, Alzheimer's Disease; MB, methylene blue; PMCA, plasma membrane Ca²⁺-ATPase; CaMBD, calmodulin binding domain

1. INTRODUCTION

Methylene blue (MB) is a cationic dye which belongs to a class of compounds known as phenothiazines. It has been used for over 100 years in a variety of applications, such as a drug in medicine (Ginimuge and Jyothi, 2010), or a histological dye in pathology, or a redox indicator in chemistry. Due to its high lipophilicity, MB has a remarkably high blood-brain barrier permeability and can reach concentrations up to hundreds of μ M in brain after intravenous or oral administration (O'Leary et al., 2010; Peter et al., 2000). In recent years, MB has attracted great interest as a potential therapeutic agent for improving memory impairment and cognition decline in aging and neurodegeneration linked to mitochondrial dysfunction (Atamna and Kumar, 2010; Zakaria et al., 2016). Furthermore, it has been proposed that MB may slow the progression of Alzheimer's disease (AD) (Oz et al., 2009). In fact, this phenothiazine and its derivative leuco-methylthioninium bis(hydromethanesulphonate (LMTM), also known as LMTX or TRx0237, have shown beneficial effects in phase II/III clinical trials in mild-moderate AD patients (Gura, 2008; Panza et al., 2016; Seripa et al., 2016; Wilcock et al., 2018; Wischik et al., 2015). Moreover, MB inhibits the in vitro aggregation of A β (Lee et al., 2017; Necula et al., 2007) and tau (Taniguchi et al., 2005), partially restores mitochondrial dysfunction and cerebral metabolism (Lin et al., 2012), and oral MB

administration to APP/PS1 mouse models of AD decreases brain A β deposition and improves cognitive impairment (Mori et al., 2014; Paban et al., 2014).

AD is the most common type of dementia among older people. It is characterized by the abundance of both extracellular amyloid plaques containing aggregates of the amyloid- β protein fragment (A β) and intracellular neurofibrillary tangles of hyperphosphorylated tau (Hardy et al., 1992; Querfurth and LaFerla, 2010). The presence of these hallmarks leads to disruption of metabolic processes, reduction of cell functions, loss of connections between cells and eventually the destruction and death of nerve cells.

Intracellular Ca²⁺ dysregulation is one of the molecular mechanisms involved in the multiple molecular events that contribute to the progression of AD (Bezprozvanny and Mattson, 2008; Brawek and Garaschuk, 2014; LaFerla, 2002; Popugaeva et al., 2017), and it has been associated to synaptic dysfunction and A β production (Anand et al., 2014; De Felice et al., 2007; Demuro et al., 2005). In AD, raises of cytosolic calcium levels stimulate the aggregation of A β (Isaacs et al., 2006; Pierrot et al., 2004; Supnet and Bezprozvanny, 2010). On the other hand, A β oligomers disturb neuronal calcium homeostasis (Lazzari et al., 2015). Besides, A β seems to affect the function of Ca²⁺-regulatory proteins. Indeed, we have already shown that A β inhibits the activity of plasma membrane Ca²⁺-ATPase (PMCA), a high affinity active transporter that pumps Ca²⁺ ions out of the cell, but does not affect activities of intracellular sarco(endo)plasmic reticulum (SERCA) and secretory pathway (SPCA) Ca²⁺-ATPases (Berrocal et al., 2009; Berrocal et al., 2012). Despite these evidences and the aforementioned studies reporting effects of MB on A β , there is a lack of knowledge concerning a functional relationship between MB and systems involved in the regulation of intracellular Ca²⁺ homeostasis.

In this work we show for the first time that MB activates the PMCA activity and also prevent and revert the A β -induced inhibition restoring the maximal velocity of PMCA. These effects were observed in membranes from control and AD-affected human brain samples, as well as in membranes expressing human PMCA isoforms and in the purified synaptosomal pig brain PMCA. Activity assays performed with truncated human PMCA isoforms indicate that the action of the MB most likely occurs by its binding to a site on PMCA close to the last transmembrane domain of the pump. Analysis of this interaction by fluorescence quenching studies revealed that MB binding

to PMCA produces a significant conformational protein change. Besides, A β seems to potentiate the affinity of the dye for the protein.

2. MATERIALS AND METHODS

Phosphatidylcholine (PC) type XI-E from egg yolk, phosphatidylserine (PS), calmodulin-agarose, methylene blue, phenothiazine and phenazine were obtained from Sigma. Phenothiazines were prepared as stock solutions of 5 mg/ml (w/v) and made freshly for each separate experiment. The full length A β peptide containing 42 amino acid residues (A β 1-42) was synthesized by StabVida. It was dissolved in 70 μ l of 1% NH₄OH to give a clear solution, and then diluted with 100 mM Hepes/KOH (pH 7.4) to prepare a 4 mg/ml stock solution. An optimal time of 2 h incubation was typically used (and referred as “aged” peptide). HiLyte™ Fluor 555 A β 1-42 was from AnaSpec. Pig brains were obtained from a local slaughterhouse and human autopsy brain tissues (medium frontal gyrus, a brain region highly affected in AD) were supplied by the Netherlands Brain Bank (Amsterdam, The Netherlands) and obtained from 8 patients diagnosed as having AD (age 79 \pm 2yr, Braak stage V/VI) and from 7 age-matched non-AD control subjects. Polyclonal anti-PMCA1, anti-PMCA2, anti-PMCA3 antibodies and monoclonal anti-PMCA4 antibody were from Thermo Scientific. The monoclonal anti-GAPDH antibody was from Santa Cruz Biotechnologies. Secondary HRP-labelled antibodies were from Sigma and from Santa Cruz Biotechnology.

2.1. Preparation of membrane extracts from cells and human brain tissues.

Native human PMCA4b (hPMCA4b) and two truncated hPMCA4b versions, the hPMCA4b-L1086* mutant, lacking 120 amino acids at the C-terminal tail, including the calmodulin-binding domain (CaMBD), and the hPMCA4b-R1052* mutant (lacking 154 amino acids at the C-terminus, including its CaMBD) were expressed in COS-7 cells as described in (Berrocal et al., 2017; Berrocal et al., 2012). Membrane extracts were prepared following the protocol described by (Sepulveda et al., 2005). Briefly, tissues were excised and cells were scraped and pelleted. Tissues and cell pellets were homogenized in 10 mM HEPES/KOH, pH 7.4; 0.32 M sucrose; 0.5 mM MgSO₄; 0.1 mM phenylmethanesulfonyl fluoride (PMSF); 2 mM 2-mercaptoethanol; and protease inhibitor cocktail solution (Roche Diagnostics, Mannheim, Germany). Homogenates were centrifuged for 10 min at 1500 g, and supernatants were centrifuged for 45 min at 100000 g. The final pellets were resuspended in 10 mM HEPES/KOH, pH 7.4 and 0.32

M sucrose, aliquoted and stored at -80°C until use. The protein content was evaluated by the Bradford method (Bradford, 1976).

2.2. Preparation of purified plasma membrane Ca^{2+} -ATPase from pig brain and yeast. The pig brain plasma membrane Ca^{2+} -ATPase (PMCA) was purified from synaptosomal plasma membrane vesicles as described in detail by (Salvador and Mata, 1996). Native hPMCA4b and truncated hPMCA4b (hPMCA4b*) version (similar to COS hPMCA4b-L1086*) were expressed and purified from *S. cerevisiae* as detailed in (Corbacho et al., 2016). Samples were stored at -80°C until use.

2.3. Western blots assays

Brain extracts were run on 7.5% SDS-PAGE gels and subsequently transferred onto nitrocellulose. After blocking, membranes were incubated overnight at 4°C with antibodies against hPMCA1, hPMCA2, rPMCA3, hPMCA4 and GAPDH, at 1:1000 dilutions. Immunoreactivity was detected with anti-mouse or anti-rabbit peroxidase-conjugates secondary antibodies (1:3000). Proteins were visualized with ECL substrate, with a ChemidocTM XRS+Imaging System (BioRad).

2.5. Ca^{2+} -ATPase activity assays

The activity was measured with a coupled enzyme assay, as described in (Salvador and Mata, 1996), in 20 μg of membrane enriched fractions isolated from post-mortem brain tissue of Alzheimer's disease patients and control subjects and from COS-7 cells overexpressing hPMCA4b isoform, or 2.5 μg of delipidated purified PMCA from pig brain and reconstituted with 13.5 μg of PC/PS (at a 80/20 weight ratio). The effect of $\text{A}\beta 1-42$ on ATPase activity was evaluated by preincubation of membranes or purified protein for 2 min at 37°C with 30 μM $\text{A}\beta 1-42$, in a final volume of 25 μl . The mixture was then diluted directly into the assay medium (50 mM Hepes/KOH (pH 7.4), 100 mM KCl, 2 mM MgCl_2 , 5 mM Na_3N , 3.16 μM free Ca^{2+} (pCa 5.5), 0.22 mM NADH, 0.42 mM phosphoenolpyruvate, 10 IU pyruvate kinase, and 28 IU lactate dehydrogenase) in 1 ml final volume. The medium assay used for membrane vesicles included 0.01% saponin (to disrupt both the plasma and intracellular membranes, allowing the access of substrates to all protein molecules in membrane vesicles). Total Ca^{2+} -ATPase activities or specific PMCA, SERCA and SPCA activities were determined in membrane

fractions as described in (Sepulveda et al., 2007). Briefly, the reaction was started with 1 mM ATP, followed by addition of MB when required. Subsequent activity measurements were done after independent additions of 100 nM thapsigargin (to inhibit SERCA activity), 2 μ M vanadate (to selectively inhibit PMCA activity) and 3 mM EGTA (to measure Mg^{2+} -ATPase activity). The activity of purified pig brain PMCA was directly measured after triggering the reaction with 1 mM ATP and, when indicated, after addition of MB at the indicated concentrations.

2.6. Fluorescence quenching assays. Fluorescence measurements were performed with a Cary Eclipse fluorescence spectrophotometer (Agilent Technologies) at 25 °C in 1 cm quartz cells with both excitation and emission slits of 10 nm. MB titrations were performed with 10 μ g of purified pig brain PMCA or purified hPMCA4b from *S.cerevisiae* or the truncated form hPMCA4b* previously incubated with A β 1-42 during 2 min when indicated. The assay was performed in a buffer containing 50 mM HEPES-KOH (pH 7.4), 100 mM KCl, 2 mM MgCl₂, and 3.16 μ M free calcium and 1 mM ATP or AMP-PNP when indicated. The fluorescence emission spectra were acquired with excitation wavelength of 270 nm for A β 1-42 or 290 nm for PMCA. Inner filter effects were corrected as indicated in (Lakowicz, 2006). Briefly, the absorbance at excitation and emission wavelengths (OD_{Exc} and OD_{Em} , respectively) of the solutions used in fluorescence measurements were measured, and then the corrected fluorescence intensity (F_{corr}) was calculated from the observed fluorescence intensity (F_{obs}) with the following equation:

$$F_{corr} = C \cdot F_{obs}, \text{ where } C = \text{antilog} [(OD_{Exc} + OD_{Em})/2].$$

In titrations with MB the sum of the increase of absorbances ($OD_{Exc} + OD_{Em}$) was always kept lower than 0.3 for all the measurements reported in this work.

Titration of 10 nM HiLyte™-Fluor555-A β 1-42 with MB were performed in a buffer containing 50 mM HEPES-KOH (pH 7.4), 100 mM KCl, 2 mM MgCl₂, 100 μ M CaCl₂ and 1 mM ATP. The fluorescence emission spectra were acquired with excitation wavelength of 525 nm. No inner filter corrections were needed in titration data, because the increase of absorbance at excitation and emission wavelengths were always <0.002. The fluorescence intensity data were corrected for volume changes during titrations, which were always <3%. Each experiment was performed in quadruplicate.

2.7. Statistical analysis

Significant differences were determined by an unpaired Student t-test with the SigmaPlot v10 software (SPSS Inc, Chicago, IL). Non-linear regression fits, statistical analysis and plotting of fluorescence assays data were done with the OriginPro 8 software. A $p \leq 0.05$ value was considered statistically significant.

3. RESULTS

3.1. Methylene blue activates the PMCA in human brain membranes affected by Alzheimer's disease and matched controls, and protects the inhibitory effect of A β .

We have previously reported that addition of A β to control brain membranes results in an altered Ca²⁺ dependence of PMCA activity that looks like that observed in AD-affected brain samples (Berrocal et al., 2009). Likely this effect could be due to the presence of toxic A β in the AD brain. In the present study we have investigated the effect of MB on total Ca²⁺-ATPase activity on membranes from AD-affected human brain membranes and age-matched control samples, in the presence and in the absence of A β 1-42 at the concentration that produces about 50% of ATPase inhibition. As shown in Fig. 1A, MB increased the ATPase activity in human control and AD brain samples in a concentration-dependent manner. The activating effect of MB was significantly higher in control (60 \pm 3%) than in AD (24.5 \pm 1.5%) samples. Remarkably, this phenothiazine could completely reverse the inhibitory effect (39.4 \pm 7.4%) exerted by 0.75 μ M A β on ATPase activity in control-membranes, reaching the same activity plateau as in the absence of the peptide. The maximal activation was achieved with 75-100 μ M MB and the MB concentration required for the half-maximal increase in activity was \sim 55 \pm 5 μ M. In this figure we also observed the lack of inhibitory effect of A β 1-42 on AD brain samples. Fig.1A also shows the lack of effect of A β in total Ca²⁺-ATPase on AD membranes as previously published (Berrocal et al., 2009). Besides, AD human brain samples always display higher Ca²⁺-ATPase activity (+33 \pm 10%) than control samples, as previously reported in Berrocal et al., 2009 (Berrocal et al., 2009). Additional control experiments performed in the absence of ATP excluded the possibility that this could be due to an enhanced contribution of NADH oxidase activity in AD brain samples (results not shown).

Total Ca²⁺-ATPase activity involves the contribution of plasma membrane PMCA and intracellular SERCA and SPCA pumps. In order to analyse if the activating

effect of MB is extensive to all Ca²⁺-ATPases or it is just specific for PMCA, functional assays were performed with MB in AD and control human brain membranes, in the presence of selective inhibitors of each Ca²⁺ pump, as described in Sepulveda et al. (Sepulveda et al., 2007). As shown in Fig. 1B, MB was able to activate the PMCA pump, reaching maximal levels of 53±1% when the protein was previously inhibited by Aβ1-42, as observed in control human samples. However, the dye did not affect the activity of both SERCA and SPCA, independently of the presence of Aβ, which does not inhibit intracellular Ca²⁺ pumps, as previously reported (Berrocal et al., 2009).

3.2. Methylene blue activates all brain PMCA isoforms expressed in COS cells and deletion of the cytosolic C-terminal domain abolishes this activation.

Western blots performed in human brain membranes with isoform-specific anti-PMCA antibodies (Fig. 2) showed that these membranes contain a mixture of PMCA isoforms, being PMCA2 and 4 more abundant than the other isoforms. In order to analyse the sensitivity of these isoforms to MB, functional assays were performed in COS membranes expressing human PMCA2 and 4 isoforms (Fig. 3). In the presence of Aβ, the hPMCA2b activity remained without any change whereas hPMCA4b activity decreased down to 40.6%, as previously reported in (Berrocal et al., 2009). However, MB increased the hPMCA2b activity up to 75.6±5%, independently of the presence of Aβ, with an EC₅₀ value around 20-25 μM. Similar activation was observed for hPMCA4b in the absence of peptide. Remarkably, MB completely reversed the Aβ inhibitory effect on hPMCA4b, reaching the same V_{max} than in the absence of peptide. Analogous effects were found for isoforms hPMCA1 and rPMCA3 (*results not shown*).

In order to shed light on the PMCA domain involved in its interaction with MB in the absence and presence of Aβ we have focused on hPMCA4b, because it is the more abundant brain PMCA isoform sensitive to inhibition by Aβ. Kinetic experiments were performed in membrane vesicles from COS cells expressing the native hPMCA4b or truncated isoforms lacking the CaMBD (hPMCA4b-L1086*) and the entire cytosolic C-domain (hPMCA4b-R1052*). As shown in Fig.4 only the intact protein was inhibited to about 59.7% by Aβ1-42 peptide, as previously reported (Berrocal et al., 2012). However, MB increased the activities of both the full-length hPMCA4b pump and the hPMCA-L1086* mutant, up to the V_{max} obtained in the absence of peptide, but it did not stimulate the activity of the shortest hPMCA4b-R1052* variant lacking the full

cytosolic C-domain. These results suggest that cytosolic C-terminal tail of PMCA is involved in its functional interaction with MB.

3.3. Methylene blue also activates the purified and reconstituted synaptosomal PMCA and protect against its inhibition by A β .

Functional assays were also done with purified synaptosomal PMCA from pig brain (Fig. 5) which has been widely characterized by our group. As already published, the purified protein is obtained in a delipidated inactivated state, but the activity is recovered after been reconstituted in phospholipids (Salvador and Mata, 1995). A mixture of PC/PS (weight ratio, 80:20) was used in this study to keep a similar composition than that of intact membranes. As shown in Fig. 5, the Ca²⁺-ATPase activity was also stimulated (up to 43.5 \pm 0.5%) by MB with an EC₅₀ between 20 and 25 μ M, and the 39.5 \pm 2 % inhibition produced by A β 1-42 was completely reversed by the phenothiazine, reaching the same V_{max} that in the absence of peptide. Addition of BSA (negative control) to the cuvette before or after MB and A β did not affect the ATPase activity and did not prevent the stimulatory effect of MB (*results not shown*).

In contrast to phenothiazine derivative MB, the pure phenothiazine and its derivative phenazine did not alter the purified PMCA activity, but they were also able to completely reverse the inhibitory effect of A β on PMCA activity and restore the activity to V_{max} values (Table I).

3.4. Analysis of methylene blue-PMCA interaction by fluorescence.

The kinetic studies shown in sections 3.1, 3.2 and 3.3, strongly suggest that MB interacts with the PMCA. However, since the PMCA undergoes cyclic changes between different conformational states during catalysis, the dissociation constant of this interaction cannot be simply derived from the activation constants obtained with the kinetic experiments. In addition, these kinetic studies cannot allow us to determine conclusively whether the ability of MB to revert the inhibition of PMCA by A β is due to MB-A β complexation or to a MB-induced conformational shift in PMCA-A β complexes. To answer these points, we have performed fluorimetric studies of the interaction of MB with purified PMCA, with A β 1-42 and with purified PMCA in the presence of A β 1-42. The PMCA used in these assays were purified from pig brain (which contains a mixture of isoforms, as shown earlier in this work) and from yeasts

expressing full-length hPMCA4b or its truncated variant, lacking the CaMBD (hPMCA4b*).

MB binding to PMCA was monitored by the quenching of the intrinsic fluorescence of PMCA (Fig. 6), which reached values equal or higher than 40% quenching for purified brain PMCA and for hPMCA4b at saturation by MB, pointing out that MB binding induces a significant conformational change in PMCA. The data obtained in the titrations of the intrinsic fluorescence with MB fit very well ($R^2 > 0.9$) to the equation for one simple binding site yielding a dissociation constant of 23 μM and 19.6 μM MB for purified brain PMCA and for hPMCA4b, respectively. Noteworthy, in the case of truncated hPMCA4b* the maximum extent of intrinsic fluorescence quenching induced by 10 μM MB decreased by 50%, whereas the dissociation constant of MB from the truncated hPMCA4b* isoform (21.1 μM MB) was only slightly higher than that obtained for full hPMCA4b. These results pointed out that cytosolic C-terminal domain of PMCA mediate the conformational change induced by the interaction of MB with PMCA. We have previously showed (Berrocal et al., 2012) that this PMCA domain is also directly involved in the interaction of A β with the PMCA. On the basis of these facts, we studied the effect of A β in the quenching of the intrinsic fluorescence of PMCA by MB. As shown in panels A and B of the Fig. 6, in the presence of 2 μM A β , i.e. an inhibitory concentration of the PMCA, the maximum extent of quenching of the intrinsic fluorescence of brain PMCA and of hPMCA4b by MB is $27.9 \pm 2.2\%$ and $29.8 \pm 0.9\%$, respectively. These values are around half the values obtained in the absence of A β . In contrast, A β was found to have no effect on the quenching of the intrinsic fluorescence of the truncated hPMCA4b* isoform by MB (Fig 6C), a result that is consistent with the loss of A β binding site in the truncated PMCA. Noteworthy, the preincubation of PMCA with 2 μM A β increased (approximately 10-fold) its binding affinity for MB, as the dissociation constant decreased from 23 to 2 μM MB for pig brain PMCA and from 19.6 to 1.9 μM MB for hPMCA4b.

It seems likely that MB forms a complex with A β , because it has been shown that photo-excited MB interacts with A β leading to its photo-oxidation (Lee et al., 2017) and that MB impairs amyloid A β oligomerization and aggregation (Lee et al., 2017; Necula et al., 2007). Therefore, we experimentally assessed this possibility by performing titration of the fluorescence of 10 nM HiLyte™ Fluor 555 A β 1-42 with MB. As shown in the Fig. 7A, MB yielded a large quenching of the fluorescence of this tagged A β ,

reaching $57 \pm 12\%$ quenching at saturation, with a dissociation constant of $0.76 \pm 0.4 \mu\text{M}$ MB. Since A β 1-42 has been shown to aggregate in the micromolar range used in kinetic experiments, we decided to experimentally assess this dissociation constant by titration of the intrinsic fluorescence of A β with MB. The MB elicited partial quenching of the intrinsic fluorescence of $10 \mu\text{M}$ A β with a dissociation constant of $1.28 \pm 0.6 \mu\text{M}$ (Fig. 7B). The inner filter effect due to the MB absorbance at 280 and 340 nm has been corrected as indicated in the Materials and Methods. Therefore, under the conditions used in Ca²⁺-ATPase assays the dissociation constant of the MB-A β complex is close to $1 \mu\text{M}$. Since preincubation of the Ca²⁺ pump with $2 \mu\text{M}$ A β increases its binding affinity for MB, in the case of purified brain PMCA (Fig. 6A) and also of the purified hPMCA4b (Fig. 6B), but not for the truncated hPMCA4b* isoform lacking the A β binding site (Fig. 6C), our results allowed to conclude that A β 1-42 binding to PMCA potentiates the binding of MB forming a ternary complex MB-(A β -PMCA).

3.5. ATP modulates the affinity of the PMCA for methylene blue.

The dissociation constant value ($1.9\text{-}2.0 \mu\text{M}$) of MB from the (A β -PMCA) complex, obtained from fluorescence measurements shown in panels A and B of Fig. 6, was much lower than the EC₅₀ values obtained for MB stimulation of the Ca²⁺-ATPase activity of purified PMCA preincubated with A β , which were around $20 \mu\text{M}$ (see Fig. 5). Considering that PMCA cycles between four major conformational states during the catalytic cycle, i.e. E1, E2, E1-P and E2-P (Brini and Carafoli, 2009; Padanyi et al., 2016), we hypothesized that there are large differences of affinity for MB between these conformational states and we performed fluorescence experiments in the absence or presence of Ca²⁺, ATP and AMP-PNP to get the effects of shifts between these conformational states on the dissociation constant of MB from brain PMCA (Fig. 8). In the presence of Ca²⁺ the PMCA is shifted towards the E1 state, while in the absence of Ca²⁺ it is in the E2 state. In the absence of nucleotide, the dissociation constant ($1\text{-}2 \mu\text{M}$) between MB and brain PMCA reconstituted in PC/PS (weight ratio, 80:20) showed similar values in the absence and in the presence of Ca²⁺, i.e. it was not significantly different between E1 and E2 PMCA conformational states. However, in the presence of 1 mM ATP, the dissociation constant values were higher, indicating that the affinity of PMCA for MB is much lower. Thus, in the presence of 1 mM ATP and the absence of Ca²⁺ (conditions at which the Ca²⁺-ATPase activity is negligible) the dissociation constant of the PMCA-MB complex is about 6-fold higher than in the absence of ATP,

and in the presence of 3.16 μM free Ca^{2+} (which favors a high Ca^{2+} -ATPase activity) it raises up to 25 ± 4 μM , i.e. it is more than 10-fold higher than in the absence of ATP and it is identical to the EC_{50} value obtained for stimulation of the Ca^{2+} -ATPase activity of purified brain PMCA (Fig. 5). This result revealed that the decrease of PMCA affinity for MB was not only due to a conformational shift to the phosphorylated states E1-P and E2-P, and suggested that at least in part it was due to ATP binding to PMCA. To experimentally assess this possibility we performed titrations of the intrinsic fluorescence of PMCA with MB in the presence of the non-hydrolysable ATP analogue AMP-PNP (adenylyl-imidodiphosphate) without or with Ca^{2+} . As shown in Fig. 8, in the presence of 1 mM AMP-PNP the dissociation constant of PMCA-MB complex is almost independent of the presence of Ca^{2+} and is very close to the dissociation constant value for the PMCA-MB complex obtained with 1 mM ATP and in the absence of Ca^{2+} .

4. DISCUSSION

Our results show that micromolar concentrations of MB stimulate the PMCA activity in all tested membranes, independently of the presence of $\text{A}\beta_{1-42}$. MB dye also prevented inhibition of PMCA by $\text{A}\beta_{1-42}$, with an EC_{50} value between 20 and 25 μM MB. As far as we know this is the first report of PMCA activation by MB and of reversion of the inhibitory effect of $\text{A}\beta$ on PMCA activity. In addition, we found that all major PMCA isoforms expressed in adult brain were stimulated to nearly the same extent by MB, a result that bears a special relevance because there are different PMCA isoforms whose expression patterns change during neuronal maturation (Guerini et al., 1999) and display regional differences in the adult brain (Marcos et al., 2009). MB concentrations as low as 5-10 μM already elicited a significant reversion of the $\text{A}\beta$ inhibition of the PMCA activity, a concentration range of MB reported to be reached in human blood plasma after intravenous bolus injection of 1.4 mg/kg MB (Aeschlimann et al., 1996). This bolus injection is within the generally accepted therapeutic bolus dose of MB, i.e. 1–2 mg/kg body weight over 10–20 min (Harvey, 1980). Pharmacokinetic studies in rodents have shown that the concentration of MB is 10–20 times higher in the brain than in the circulation one hour following systemic administration, indicating a rapid and extensive accumulation of MB in the nervous system (Kristiansen, 1989; Peter et al., 2000). Furthermore, MB has been shown to pass the blood-brain barrier, when administered intraperitoneally (O'Leary et al., 1968). On these grounds, the results reported in this work open new pharmacological insights for the therapeutic use of MB

and other phenothiazine derivatives in AD (and other amyloid neurodegenerative diseases), because intracellular calcium homeostasis has been shown to be disrupted in both sporadic and familial forms of AD (Berridge, 2014; LaFerla, 2002; Popugaeva et al., 2017), and PMCA activity plays a major role for the maintenance of neuronal cytosolic calcium homeostasis within the range required for neuronal survival (Berridge, 2014; Brini et al., 2017; Kurnellas et al., 2005). Moreover, the EC₅₀ of PMCA stimulation by MB falls well below 100 μM, which is the lower MB concentration for which toxic effects have been reported in preclinical *in vitro* studies (Oz et al., 2011).

In this work we have found that phenothiazine or phenazine, whose structures do not contain a substituent on the tricyclic ring, did not affect PMCA activity but they completely abolished the inhibitory action of Aβ. However, the MB, which contains dimethyl amino groups at positions 3 and 7 of the phenothiazine ring, activated the PMCA activity in the absence and presence of Aβ peptide. It is worthy to note here that previous work performed with phenothiazine derivatives such as thioridazine, chlorpromazine or fluphenazine, which contain an alkyl bridge connecting the nitrogen atom at position 10 (N-10) of the tricyclic ring of phenothiazine inhibited the PMCA activity but increased Ca²⁺ transport (Palacios et al., 2004). Therefore, we conclude that the effects of phenothiazine derivatives on PMCA are tightly dependent upon chemical substituents of their chemical structures. In this respect, several authors have already reported that substituents on the C-2 of the tricyclic phenothiazine ring and the length of the alkyl bridge substituent on N-10 are determinant factors on the activity of phenothiazines against cancer cells (Ford et al., 1989; Jaszczyszyn et al., 2012; Pajeva and Wiese, 1997; Pajeva et al., 1996; Ramu and Ramu, 1992).

Our results also show that among the calcium pumps known to be present in neurons (PMCA, SERCA and SPCA) only PMCA is stimulated by MB. Noteworthy, the major structural difference between these calcium pumps is the long C-terminal tail which is present in PMCA, but not in the other calcium pumps, and in previous works we have shown that Aβ binds to a site within this C-terminal domain of the PMCA (Berrocal et al., 2012).

The interaction of MB with PMCA has been experimentally assessed and quantified by quenching studies using intrinsic tryptophan fluorescence of PMCA purified from pig brain and of two yeast-expressed purified variants of hPMCA4b (the Aβ-sensitive PMCA isoform most heavily expressed in brain samples), the full-length

hPMCA4b and the truncated hPMCA4b* lacking the C-terminal CaMBD, which also have lost the sensitivity to inhibition by A β (Berrocal et al., 2012; Mata, 2018). Results showed that, at saturation, MB binding to purified pig brain PMCA or to hPMCA4b produced more than 40% quenching of intrinsic PMCA fluorescence. This finding suggests that MB binding induces a significant conformational change in these proteins, yielding a dissociation constant close the EC₅₀ value obtained in each case from PMCA activity titration with MB, i.e. ~20-25 μ M MB. The C-terminal tail of the PMCA plays a major role in this conformational change, because deletion of the CaMBD sequence of this domain produced nearly 50% reduction of the quenching of PMCA intrinsic fluorescence elicited by MB binding. The fact that MB activated both, the intact protein and the truncated form lacking the CaMBD, but not the shortest form lacking the whole C-terminal tail, suggests that MB binds to protein residues located in the C-terminal site close to the CaMBD. Consistent with this result, deletion of the CaMBD portion of the C-terminal domain of hPMCA4b did not significantly alter the dissociation constant of MB from the hPMCA4b, implying that the MB binding site on PMCA is interacting or structurally connected with the CaMBD and that this interaction results in a conformational change of PMCA. This point was confirmed by the effects of preincubation of PMCA with 2 μ M A β 1-42 on the quenching of the intrinsic fluorescence of PMCA by MB. Preincubation of the truncated hPMCA4b* with A β 1-42 did not alter the quenching afforded by titration with MB in contrast with the major alterations observed with native hPMCA4b and with pig brain PMCA. Moreover, in the presence of A β the affinity of MB for pig brain PMCA and for hPMCA4b is largely increased since the dissociation constant decreased approximately 10-fold in both cases, but not for the truncated hPMCA4b* isoform. Indeed, MB not only reversed the inhibitory effect of A β on PMCA, but it also fully activated the protein to a level similar to that attained in the absence of A β . This suggests that MB can bind simultaneously to both, A β and PMCA. While the alteration of the quenching of intrinsic fluorescence attained at saturation of MB by preincubation of PMCA with A β 1-42 is an expected outcome if A β and MB binding sites are located in different but interacting or structurally connected domains, the increase of affinity for MB suggested the possibility that A β may provide an additional and stronger linkage to MB in the (A β -PMCA) complex. Titration of A β 1-42 fluorescence with MB confirmed this point, as it yielded an average dissociation constant of 0.8-1.3 μ M MB for the complex MB-A β which is close to the dissociation constant obtained for MB from the (A β -PMCA) complex,

namely, 1.9-2.0 μM MB. Thus, the presence of 2 μM $\text{A}\beta$ leads to an increase of MB affinity for PMCA, therefore the amyloid- β peptide potentiates the stimulating effect of MB on PMCA function. It is worth noting that submicromolar to micromolar concentrations of $\text{A}\beta$ have been reported to be locally reached in the brain of AD patients (Cherny et al., 1999), a concentration range of $\text{A}\beta$ which leads to $\text{A}\beta$ fibrils formation *in vitro* (Walsh et al., 1999). This suggests that in these AD patients, the presence of $\text{A}\beta$ could up-modulate the stimulating effect of MB on the PMCA role as a fine modulator of cytosolic calcium levels.

The 10-fold difference between the dissociation constant (1.9-2.0 μM) of MB from the ($\text{A}\beta$ -PMCA) complex obtained from titration with MB of the intrinsic fluorescence of PMCA and the EC_{50} value (~ 20 μM) for PMCA activity stimulation by MB, deserves to be rationalized. Our results have shown that the presence of millimolar ATP concentrations in the assay medium can account for a 10-fold decrease of the affinity of PMCA for MB. As the presence of ATP and absence of calcium or the presence of the non-hydrolyzable ATP analogue AMP-PNP can account for ~ 5 -fold decrease of the affinity of PMCA for MB, we conclude that steric hindrance by ATP binding contributes to half of the observed decrease of PMCA affinity for MB. Therefore, PMCA phosphorylation should produce a further 2-fold decrease of PMCA affinity for MB. Then, it is likely that MB binding to a specific site on the C-terminal domain also implies its interaction with a place close to the nucleotide binding site in the catalytic region of PMCA, a domain that has been shown to be modulated by interactions with the CaMBD (Brini and Carafoli, 2009; Di Leva et al., 2008), a region which also interacts with $\text{A}\beta$ (Corbacho et al., 2017). The cross-modulation between ATP and MB binding to PMCA suggests that a decrease of the cellular energy charge due to cellular ATP depletion can alter the EC_{50} of MB-stimulated PMCA activity. Since an altered mitochondrial bioenergetics has been shown to mediate neuronal death in a large number of neurodegenerative processes (Beal, 2002; Beal et al., 2000), this bears potential pharmacological value for the therapeutic treatment of all of them, not only for AD treatment.

CONCLUSIONS

In summary, the MB effect on PMCA not only on the protein itself but also related to the neurotoxic $\text{A}\beta$, opens new pharmacological perspectives due to its ability to induce a conformational change on the protein that enhances its function as a

cytosolic Ca^{2+} modulator, thus, stimulating its physiological key role to remove the excess of calcium accumulated in the cytosol in neurodegenerative pathologies.

ACKNOWLEDGEMENTS

We want to thank Dr. Jesús Avila (CBMSO, Madrid, Spain) for his help in obtaining human brain tissue.

FUNDING: This work was supported by the Spanish Ministerio de Economía y Competitividad, MINECO, Madrid, Spain (grant numbers BFU2014-53641-P, BFU2017-85723-P); and by the Junta de Extremadura (GR15139, Research group BBB008). Both grants were co-financed by FEDER Funds.

Declaration of interests

The authors declare they have not conflicts of interest.

Author's contribution

M.B. performed most of the experimental work and I.C. contributed to fluorescence experiments. All authors analyzed and discussed the results. C.G-M and A-M.M. also designed the experiments, and wrote the manuscript. All authors revised and approved the final manuscript.

FIGURE LEGENDS

Fig.1: Effects of $\text{A}\beta$ 1-42 and/or MB on Ca^{2+} -ATPase activity in membranes from human control (HC, \circ ●) and AD affected (HAD, \triangle ▲) brains samples. A) Membranes (10 μg) were incubated as previously described without (open symbols) or with (filled symbols) 30 μM $\text{A}\beta$ 1-42 in 25 μl and diluted up to 1 ml final volume with the assay medium which also contained 0.01% saponin (to disrupt both the plasma and intracellular membranes, allowing the access of substrates to all protein molecules in membrane vesicles). Activities were assayed after triggering the reaction with 1 mM ATP followed by addition of indicated concentrations of MB. B) Subsequent activity measurements were done after independent additions of 100 nM thapsigargin, 2 μM vanadate and 3 mM EGTA, in order to measure the contribution of PMCA, SERCA and SPCA activities to total Ca^{2+} -ATPase activity. Data show activity values obtained with

100 μM of MB and are expressed in $\mu\text{mol}/\text{min}/\text{mg}$ protein mean $\pm\text{SE}$ of four experiments performed with three preparations. * $P < 0.001$ vs. control.

Fig.2: Diversity of PMCA isoforms in membrane vesicles of human brain.

Representative western blots performed in triplicated with three different membrane samples from human medium frontal gyrus and stained with PMCA isoform-specific antibodies. The anti-GAPDH antibody was used as protein loading control to quantify relative PMCA levels. Data are presented as mean \pm SE relative values (arbitrary units).

Fig.3: Activating effect of MB on hPMCA2b and hPMCA4b isoforms.

Ten μg of membranes from COS cells overexpressing hPMCA2b and hPMCA4b isoforms were incubated without (open symbols) or with (filled symbols) 30 μM A β 1-42 in 25 μl and diluted up to 1 ml final volume with the assay medium which also contained 0.01% saponin. Activity was measured after addition of 1 mM ATP and sequential additions of MB as indicated. Results are expressed in $\mu\text{mol}/\text{min}/\text{mg}$ protein mean $\pm\text{SE}$ of four experiments performed with three preparations.

Fig.4: The activities of intact and truncated hPMCA4b isoforms are differentially regulated by A β and MB.

Membranes (10 μg) prepared from COS-7 cells overexpressing the native human PMCA4b and truncated hPMCA4b-L1086* and hPMCA4b-R1052* isoforms were incubated as previously described, without (white bars) or with 30 μM A β 1-42 (grey bars). Activities were assayed by successive additions of 1 mM ATP and 100 μM MB (striped bars) as indicated and are expressed in $\mu\text{mol}/\text{min}/\text{mg}$ protein mean $\pm\text{SE}$ of four experiments performed with three preparations. * $P < 0.001$ vs. control.

Fig.5: MB activates Ca $^{2+}$ -ATPase activity and reverses the inhibitory effect of A β peptide on the purified synaptosomal PMCA.

Purified PMCA from pig brain (2.5 μg) was mixed with a 13.3 μg of PC/PS mixture in a 80/20 ratio, and incubated for 2 min at 37 $^{\circ}\text{C}$ in the absence (\circ) or presence (\bullet) of 30 μM aged A β 1-42, in a 25 μl total volume, followed by addition of up to 1 ml assay medium. The Ca $^{2+}$ -ATPase activity was measured as described in the Methods, triggering the reaction with 1 mM ATP. Titrations were performed by successive additions of MB to give the indicated

concentrations. Activity values are expressed in $\mu\text{mol}/\text{min}/\text{mg}$ protein mean \pm SE of eight experiments performed with four preparations.

Fig.6: A β modulates PMCA-MB interaction. Fluorescence quenching by titration with MB of 10 μg of purified PMCA from pig brain (A) or purified hPMCA4b expressed in *S. cerevisiae* as the native form (B) or as its truncated variant hPMCA4b*, lacking the CaMBD (C), before (open symbols) and after (closed symbols) previous incubation with 2 μM A β 1-42. Assays were performed as indicated in the Materials and Methods. The non-linear regression analysis of MB quenching titration data (excitation and emission wavelengths: 290 and 340 nm, respectively) fit well to a one binding site ($R^2 > 0.9$). The inner filter effect due to the MB absorbance at 280 and 340 nm has been corrected as indicated in the Materials and Methods. Data shown are means \pm SE of titration data of three experiments performed with three preparations.

Fig.7: Fluorescence quenching by MB of HiLyte™ fluor 555 A β 1-42 (FluorA β) and of non-fluorescent A β (Non-fluor A β). Non-linear regression analysis of fluorescence quenching of 10 nM FluorA β (A) and 10 μM Non-fluor A β (B) by MB titration. Data were acquired with excitation and emission wavelengths of 525 and 573 nm (Panel A), 270 nm, and 310 nm (Panel B), respectively, and fit well to one binding site equation ($R^2 > 0.9$). Data shown are means \pm SE of titration data of three experiments performed with three preparations. The inserts show fluorescence emission spectra of FluorA β (A) or Non-fluor A β (B) sequentially acquired in the absence and presence of increasing concentrations of MB, for additional experimental details see the Materials and Methods.

Fig.8: Effects of nucleotides and Ca²⁺ in the affinity of PMCA for MB. The dissociation constant (Kd) of MB-PMCA was obtained by titration of the intrinsic fluorescence of 10 μg purified pig brain PMCA (excitation and emission wavelengths: 290 and 340 nm, respectively) with MB, in the absence and presence of 3.16 μM free calcium and in the absence or presence of 1 mM of ATP or AMP-PNP, as indicated. Statistical significant differences with respect to the Kd obtained in the absence of nucleotide (*, $p < 0.05$) and with respect to the Kd obtained with both, ATP and Ca²⁺ (+, $p < 0.05$).

- Aeschlimann, C., Cerny, T., Kupfer, A., 1996. Inhibition of (mono)amine oxidase activity and prevention of ifosfamide encephalopathy by methylene blue. *Drug Metab Dispos* 24, 1336-1339.
- Anand, R., Gill, K. D., Mahdi, A. A., 2014. Therapeutics of Alzheimer's disease: Past, present and future. *Neuropharmacology* 76 Pt A, 27-50.
- Atamna, H., Kumar, R., 2010. Protective role of methylene blue in Alzheimer's disease via mitochondria and cytochrome c oxidase. *J Alzheimers Dis* 20 Suppl 2, S439-452.
- Beal, M. F., 2002. Oxidatively modified proteins in aging and disease. *Free Radic Biol Med* 32, 797-803.
- Beal, M. F., Palomo, T., Kostrzewa, R. M., Archer, T., 2000. Neuroprotective and neurorestorative strategies for neuronal injury. *Neurotox Res* 2, 71-84.
- Berridge, M. J., 2014. Calcium regulation of neural rhythms, memory and Alzheimer's disease. *J Physiol* 592, 281-293.
- Berrocal, M., Corbacho, I., Sepulveda, M. R., Gutierrez-Merino, C., Mata, A. M., 2017. Phospholipids and calmodulin modulate the inhibition of PMCA activity by tau. *Biochim Biophys Acta* 1864, 1028-1035.
- Berrocal, M., Marcos, D., Sepulveda, M. R., Perez, M., Avila, J., Mata, A. M., 2009. Altered Ca^{2+} dependence of synaptosomal plasma membrane Ca^{2+} -ATPase in human brain affected by Alzheimer's disease. *FASEB J* 23, 1826-1834.
- Berrocal, M., Sepulveda, M. R., Vazquez-Hernandez, M., Mata, A. M., 2012. Calmodulin antagonizes amyloid-beta peptides-mediated inhibition of brain plasma membrane Ca^{2+} -ATPase. *Biochim Biophys Acta* 1822, 961-969.
- Bezprozvanny, I., Mattson, M. P., 2008. Neuronal calcium mishandling and the pathogenesis of Alzheimer's disease. *Trends Neurosci* 31, 454-463.
- Bradford, M. M., 1976. A rapid and sensitive method for the quantitation of microgram quantities of protein utilizing the principle of protein-dye binding. *Anal Biochem* 72, 248-254.
- Brawek, B., Garaschuk, O., 2014. Network-wide dysregulation of calcium homeostasis in Alzheimer's disease. *Cell Tissue Res* 357, 427-438.
- Brini, M., Carafoli, E., 2009. Calcium pumps in health and disease. *Physiol Rev* 89, 1341-1378.
- Brini, M., Carafoli, E., Cali, T., 2017. The plasma membrane calcium pumps: focus on the role in (neuro)pathology. *Biochem Biophys Res Commun* 483, 1116-1124.
- Corbacho, I., Berrocal, M., Torok, K., Mata, A. M., Gutierrez-Merino, C., 2017. High affinity binding of amyloid beta-peptide to calmodulin: Structural and functional implications. *Biochem Biophys Res Commun* 486, 992-997.
- Corbacho, I., Garcia-Prieto, F. F., Hinojosa, A. E., Berrocal, M., Mata, A. M., 2016. An improved method for expression and purification of functional human Ca^{2+} transporter PMCA4b in *Saccharomyces cerevisiae*. *Protein Expr Purif* 120, 51-58.
- Cherny, R. A., Legg, J. T., McLean, C. A., Fairlie, D. P., Huang, X., Atwood, C. S., Beyreuther, K., Tanzi, R. E., Masters, C. L., Bush, A. I., 1999. Aqueous dissolution of Alzheimer's disease A β amyloid deposits by biometal depletion. *J Biol Chem* 274, 23223-23228.
- De Felice, F. G., Velasco, P. T., Lambert, M. P., Viola, K., Fernandez, S. J., Ferreira, S. T., Klein, W. L., 2007. A β oligomers induce neuronal oxidative stress through an N-methyl-D-aspartate receptor-dependent mechanism that is blocked by the Alzheimer drug memantine. *J Biol Chem* 282, 11590-11601.
- Demuro, A., Mina, E., Kaye, R., Milton, S. C., Parker, I., Glabe, C. G., 2005. Calcium dysregulation and membrane disruption as a ubiquitous neurotoxic mechanism of soluble amyloid oligomers. *J Biol Chem* 280, 17294-17300.

- Di Leva, F., Domi, T., Fedrizzi, L., Lim, D., Carafoli, E., 2008. The plasma membrane Ca^{2+} ATPase of animal cells: structure, function and regulation. *Arch Biochem Biophys* 476, 65-74.
- Ford, J. M., Prozialeck, W. C., Hait, W. N., 1989. Structural features determining activity of phenothiazines and related drugs for inhibition of cell growth and reversal of multidrug resistance. *Mol. Pharmacol.* 35, 105-115.
- Ginimuge, P. R., Jyothi, S. D., 2010. Methylene blue: revisited. *J Anaesthesiol Clin Pharmacol* 26, 517-520.
- Guerini, D., Garcia-Martin, E., Gerber, A., Volbracht, C., Leist, M., Merino, C. G., Carafoli, E., 1999. The expression of plasma membrane Ca^{2+} pump isoforms in cerebellar granule neurons is modulated by Ca^{2+} . *J Biol Chem* 274, 1667-1676.
- Gura, T., 2008. Hope in Alzheimer's fight emerges from unexpected places. *Nat Med* 14, 894.
- Hardy, J., Chartier-Harlin, M. C., Mullan, M., 1992. Alzheimer disease: the new agenda. *Am J Hum Genet* 50, 648-651.
- Harvey, D. J., 1980. Vinyltrimethylsilyl ethers as derivatives for the characterization of steroids and cannabinoids by gas chromatography mass spectrometry. *Biomed Mass Spectrom* 7, 211-216.
- Isaacs, A. M., Senn, D. B., Yuan, M., Shine, J. P., Yankner, B. A., 2006. Acceleration of amyloid beta-peptide aggregation by physiological concentrations of calcium. *J Biol Chem* 281, 27916-27923.
- Jaszczyszyn, A., Gasiorowski, K., Swiatek, P., Malinka, W., Cieslik-Boczula, K., Petrus, J., Czarnik-Matusiewicz, B., 2012. Chemical structure of phenothiazines and their biological activity. *Pharmacol Rep* 64, 16-23.
- Kristiansen, J. E., 1989. Dyes, antipsychotic drugs, and antimicrobial activity. Fragments of a development, with special reference to the influence of Paul Ehrlich. *Dan Med Bull* 36, 178-185.
- Kurnellas, M. P., Nicot, A., Shull, G. E., Elkabes, S., 2005. Plasma membrane calcium ATPase deficiency causes neuronal pathology in the spinal cord: a potential mechanism for neurodegeneration in multiple sclerosis and spinal cord injury. *FASEB J* 19, 298-300.
- LaFerla, F. M., 2002. Calcium dyshomeostasis and intracellular signalling in Alzheimer's disease. *Nat Rev Neurosci* 3, 862-872.
- Lakowicz, J., 2006. *Principles of Fluorescence Spectroscopy*. Kluwer/Plenum, New York.
- Lazzari, C., Kipanyula, M. J., Agostini, M., Pozzan, T., Fasolato, C., 2015. Abeta42 oligomers selectively disrupt neuronal calcium release. *Neurobiol Aging* 36, 877-885.
- Lee, B. I., Suh, Y. S., Chung, Y. J., Yu, K., Park, C. B., 2017. Shedding Light on Alzheimer's beta-Amyloidosis: Photosensitized Methylene Blue Inhibits Self-Assembly of beta-Amyloid Peptides and Disintegrates Their Aggregates. *Sci Rep* 7, 7523.
- Marcos, D., Sepulveda, M. R., Berrocal, M., Mata, A. M., 2009. Ontogeny of ATP hydrolysis and isoform expression of the plasma membrane Ca^{2+} -ATPase in mouse brain. *BMC Neurosci* 10, 112.
- Mata, A. M., 2018. Functional interplay between plasma membrane Ca^{2+} -ATPase, amyloid beta-peptide and tau. *Neurosci Lett* 663, 55-59.
- Mori, T., Koyama, N., Segawa, T., Maeda, M., Maruyama, N., Kinoshita, N., Hou, H., Tan, J., Town, T., 2014. Methylene blue modulates beta-secretase, reverses cerebral amyloidosis, and improves cognition in transgenic mice. *J Biol Chem* 289, 30303-30317.

- Necula, M., Breydo, L., Milton, S., Kayed, R., van der Veer, W. E., Tone, P., Glabe, C. G., 2007. Methylene blue inhibits amyloid Abeta oligomerization by promoting fibrillization. *Biochemistry* 46, 8850-8860.
- O'Leary, J. C., 3rd, Li, Q., Marinec, P., Blair, L. J., Congdon, E. E., Johnson, A. G., Jinwal, U. K., Koren, J., 3rd, Jones, J. R., Kraft, C., Peters, M., Abisambra, J. F., Duff, K. E., Weeber, E. J., Gestwicki, J. E., Dickey, C. A., 2010. Phenothiazine-mediated rescue of cognition in tau transgenic mice requires neuroprotection and reduced soluble tau burden. *Mol Neurodegener* 5, 45.
- O'Leary, J. L., Petty, J., Harris, A. B., Inukai, J., 1968. Supravital staining of mammalian brain with intra-arterial methylene blue followed by pressurized oxygen. *Stain Technol* 43, 197-201.
- Oz, M., Lorke, D. E., Hasan, M., Petroianu, G. A., 2011. Cellular and molecular actions of Methylene Blue in the nervous system. *Med Res Rev* 31, 93-117.
- Oz, M., Lorke, D. E., Petroianu, G. A., 2009. Methylene blue and Alzheimer's disease. *Biochem Pharmacol* 78, 927-932.
- Paban, V., Manrique, C., Filali, M., Maunoir-Regimbal, S., Fauvelle, F., Alescio-Lautier, B., 2014. Therapeutic and preventive effects of methylene blue on Alzheimer's disease pathology in a transgenic mouse model. *Neuropharmacology* 76 Pt A, 68-79.
- Padanyi, R., Paszty, K., Hegedus, L., Varga, K., Papp, B., Penniston, J. T., Enyedi, A., 2016. Multifaceted plasma membrane Ca^{2+} pumps: From structure to intracellular Ca^{2+} handling and cancer. *Biochim Biophys Acta* 1863, 1351-1363.
- Pajeva, I. K., Wiese, M., 1997. QSAR and Molecular Modelling of Catamphiphilic Drugs Able to Modulate Multidrug Resistance in Tumors. *Quantitative Structure-Activity Relationships* 16, 1-10.
- Pajeva, I. K., Wiese, M., Cordes, H. P., Seydel, J. K., 1996. Membrane interactions of some catamphiphilic drugs and relation to their multidrug-resistance-reversing ability. *J Cancer Res Clin Oncol* 122, 27-40.
- Palacios, J., Sepulveda, M. R., Lee, A. G., Mata, A. M., 2004. Ca^{2+} transport by the synaptosomal plasma membrane Ca^{2+} -ATPase and the effect of thioridazine. *Biochemistry* 43, 2353-2358.
- Panza, F., Solfrizzi, V., Seripa, D., Imbimbo, B. P., Lozupone, M., Santamato, A., Zecca, C., Barulli, M. R., Bellomo, A., Pilotto, A., Daniele, A., Greco, A., Logroscino, G., 2016. Tau-Centric Targets and Drugs in Clinical Development for the Treatment of Alzheimer's Disease. *Biomed Res Int* 2016, 3245935.
- Peter, C., Hongwan, D., Kupfer, A., Lauterburg, B. H., 2000. Pharmacokinetics and organ distribution of intravenous and oral methylene blue. *Eur J Clin Pharmacol* 56, 247-250.
- Pierrot, N., Ghisdal, P., Caumont, A. S., Octave, J. N., 2004. Intraneuronal amyloid-beta1-42 production triggered by sustained increase of cytosolic calcium concentration induces neuronal death. *J Neurochem* 88, 1140-1150.
- Popugaeva, E., Pchitskaya, E., Bezprozvanny, I., 2017. Dysregulation of neuronal calcium homeostasis in Alzheimer's disease - A therapeutic opportunity? *Biochem Biophys Res Commun* 483, 998-1004.
- Querfurth, H. W., LaFerla, F. M., 2010. Alzheimer's disease. *N Engl J Med* 362, 329-344.
- Ramu, A., Ramu, N., 1992. Reversal of multidrug resistance by phenothiazines and structurally related compounds. *Cancer Chemother Pharmacol* 30, 165-173.
- Salvador, J. M., Mata, A. M., 1995. Identification of two types of Ca^{2+} transport ATPases in pig brain by specific antibodies. *Biochem Soc Trans* 23, 571S.

- Salvador, J. M., Mata, A. M., 1996. Purification of the synaptosomal plasma membrane ($\text{Ca}^{2+} + \text{Mg}^{2+}$)-ATPase from pig brain. *Biochem J* 315 (Pt 1), 183-187.
- Sepulveda, M. R., Berrocal, M., Marcos, D., Wuytack, F., Mata, A. M., 2007. Functional and immunocytochemical evidence for the expression and localization of the secretory pathway Ca^{2+} -ATPase isoform 1 (SPCA1) in cerebellum relative to other Ca^{2+} pumps. *J Neurochem* 103, 1009-1018.
- Sepulveda, M. R., Hidalgo-Sanchez, M., Mata, A. M., 2005. A developmental profile of the levels of calcium pumps in chick cerebellum. *J Neurochem* 95, 673-683.
- Sepulveda, M. R., Mata, A. M., 2004. The interaction of ethanol with reconstituted synaptosomal plasma membrane Ca^{2+} -ATPase. *Biochim Biophys Acta* 1665, 75-80.
- Seripa, D., Solfrizzi, V., Imbimbo, B. P., Daniele, A., Santamato, A., Lozupone, M., Zuliani, G., Greco, A., Logroscino, G., Panza, F., 2016. Tau-directed approaches for the treatment of Alzheimer's disease: focus on leuco-methylthionium. *Expert Rev Neurother* 16, 259-277.
- Supnet, C., Bezprozvanny, I., 2010. The dysregulation of intracellular calcium in Alzheimer disease. *Cell Calcium* 47, 183-189.
- Taniguchi, S., Suzuki, N., Masuda, M., Hisanaga, S., Iwatsubo, T., Goedert, M., Hasegawa, M., 2005. Inhibition of heparin-induced tau filament formation by phenothiazines, polyphenols, and porphyrins. *J Biol Chem* 280, 7614-7623.
- Walsh, D. M., Hartley, D. M., Kusumoto, Y., Fezoui, Y., Condron, M. M., Lomakin, A., Benedek, G. B., Selkoe, D. J., Teplow, D. B., 1999. Amyloid beta-protein fibrillogenesis. Structure and biological activity of protofibrillar intermediates. *J Biol Chem* 274, 25945-25952.
- Wilcock, G. K., Gauthier, S., Frisoni, G. B., Jia, J., Hardlund, J. H., Moebius, H. J., Bentham, P., Kook, K. A., Schelter, B. O., Wischik, D. J., Davis, C. S., Staff, R. T., Vuksanovic, V., Ahearn, T., Bracoud, L., Shamsi, K., Marek, K., Seibyl, J., Riedel, G., Storey, J. M. D., Harrington, C. R., Wischik, C. M., 2018. Potential of Low Dose Leuco-Methylthionium Bis(Hydromethanesulphonate) (LMTM) Monotherapy for Treatment of Mild Alzheimer's Disease: Cohort Analysis as Modified Primary Outcome in a Phase III Clinical Trial. *J Alzheimers Dis* 61, 435-457.
- Wischik, C. M., Staff, R. T., Wischik, D. J., Bentham, P., Murray, A. D., Storey, J. M., Kook, K. A., Harrington, C. R., 2015. Tau aggregation inhibitor therapy: an exploratory phase 2 study in mild or moderate Alzheimer's disease. *J Alzheimers Dis* 44, 705-720.
- Zakaria, A., Hamdi, N., Abdel-Kader, R. M., 2016. Methylene Blue Improves Brain Mitochondrial ABAD Functions and Decreases Abeta in a Neuroinflammatory Alzheimer's Disease Mouse Model. *Mol Neurobiol* 53, 1220-1228.

Table 1: Effects of phenothiazine derivatives (100 μM) on purified pig brain PMCA activity in the absence and presence of 0.75 μM A β 1-42

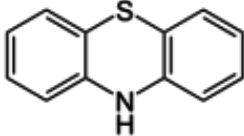
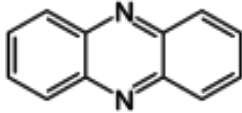
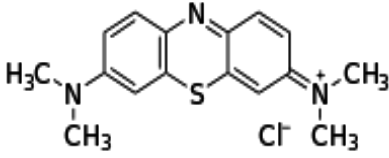
	Activity ($\mu\text{mol}\cdot\text{min}^{-1}\cdot\text{mg}^{-1}$)
Control	1.30 \pm 0.08 (100%)
A β	0.64 \pm 0.05 (49.2 %)
Phenothiazine	1.20 \pm 0.03 (92.3 %)
 A β + phenothiazine	1.25 \pm 0.06 (96.1 %)
Phenazine	1.40 \pm 0.08 (107.7 %)
 A β + phenazine	1.37 \pm 0.06 (105.4 %)
Methylene blue	1.73 \pm 0.07 (133 %)
 A β + methylene blue	1.67 \pm 0.09 (128.4 %)

Figure 1
[Click here to download high resolution image](#)

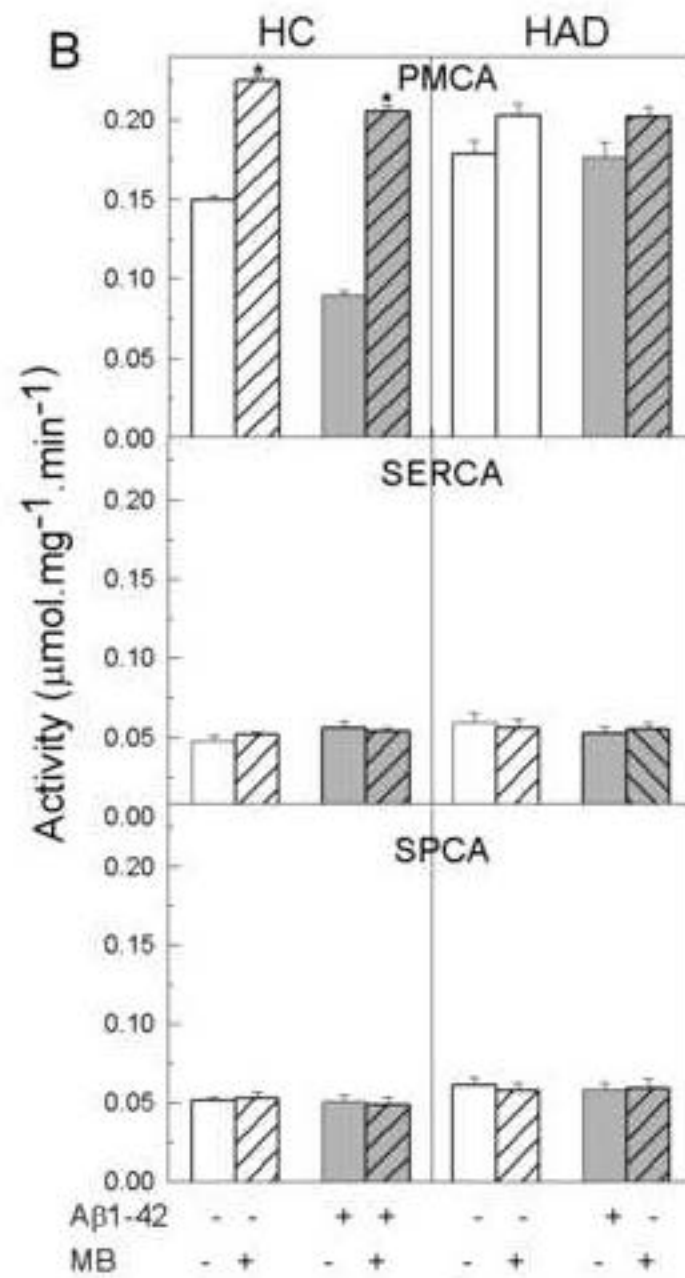
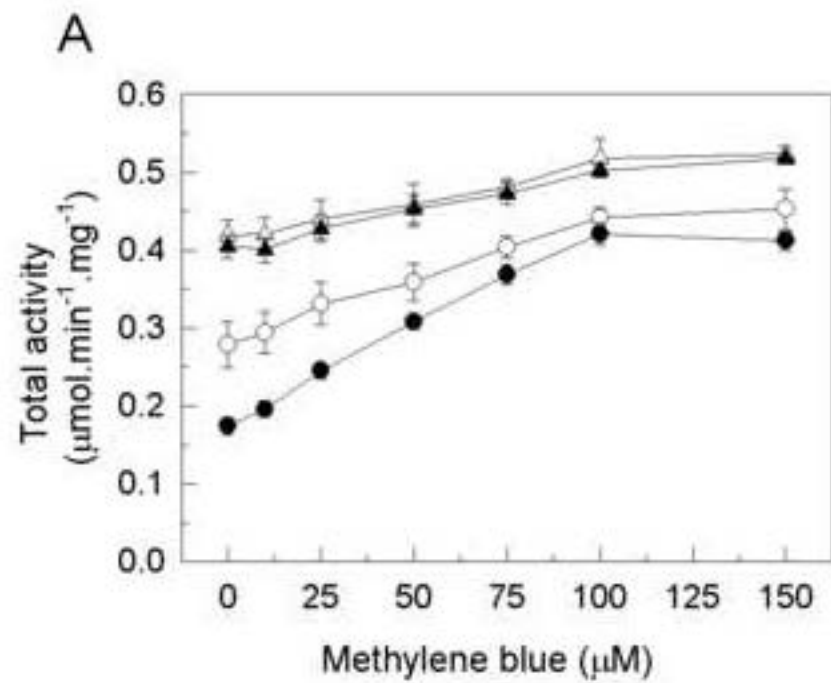


Figure 2
[Click here to download high resolution image](#)

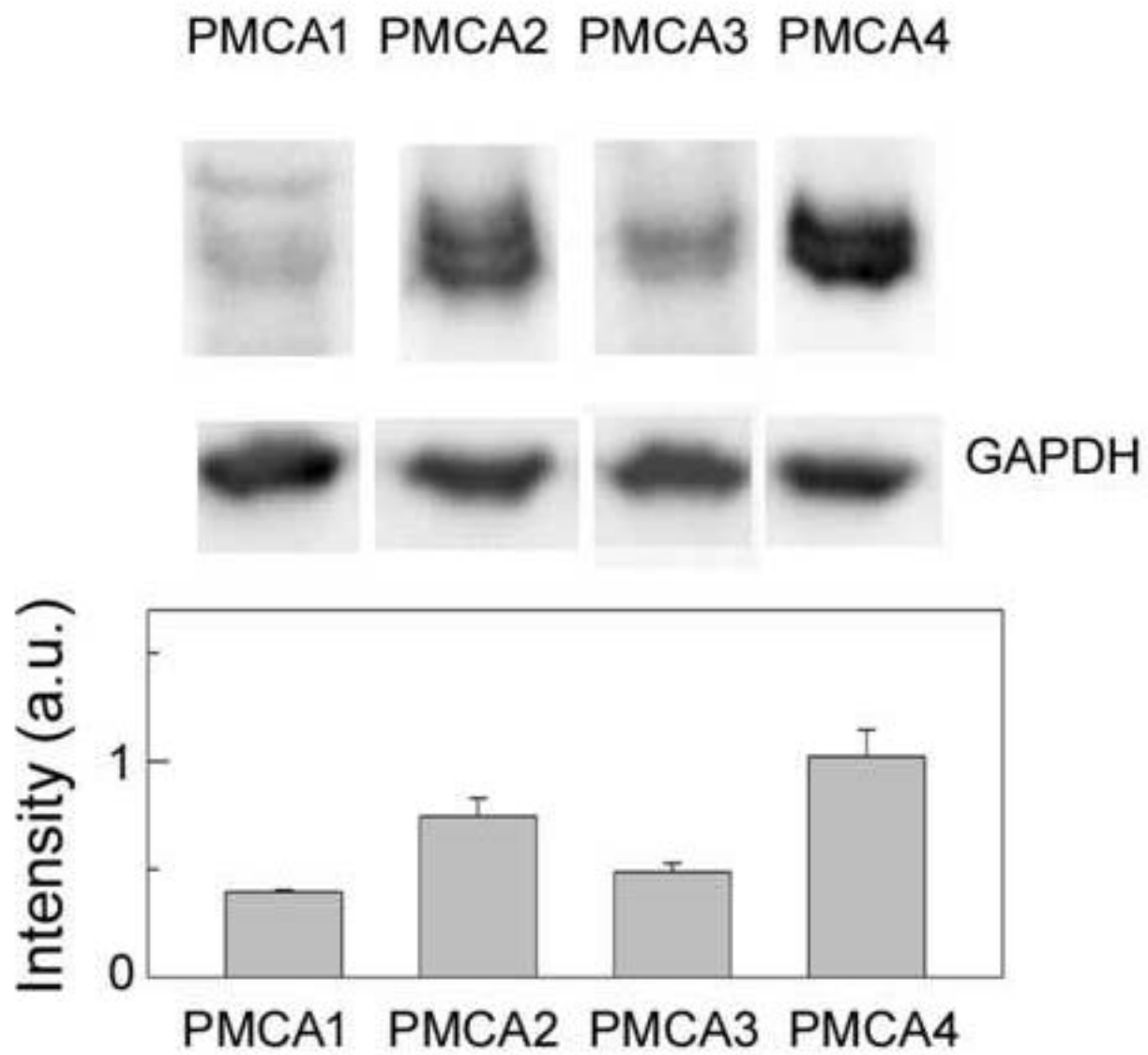


Figure 3
[Click here to download high resolution image](#)

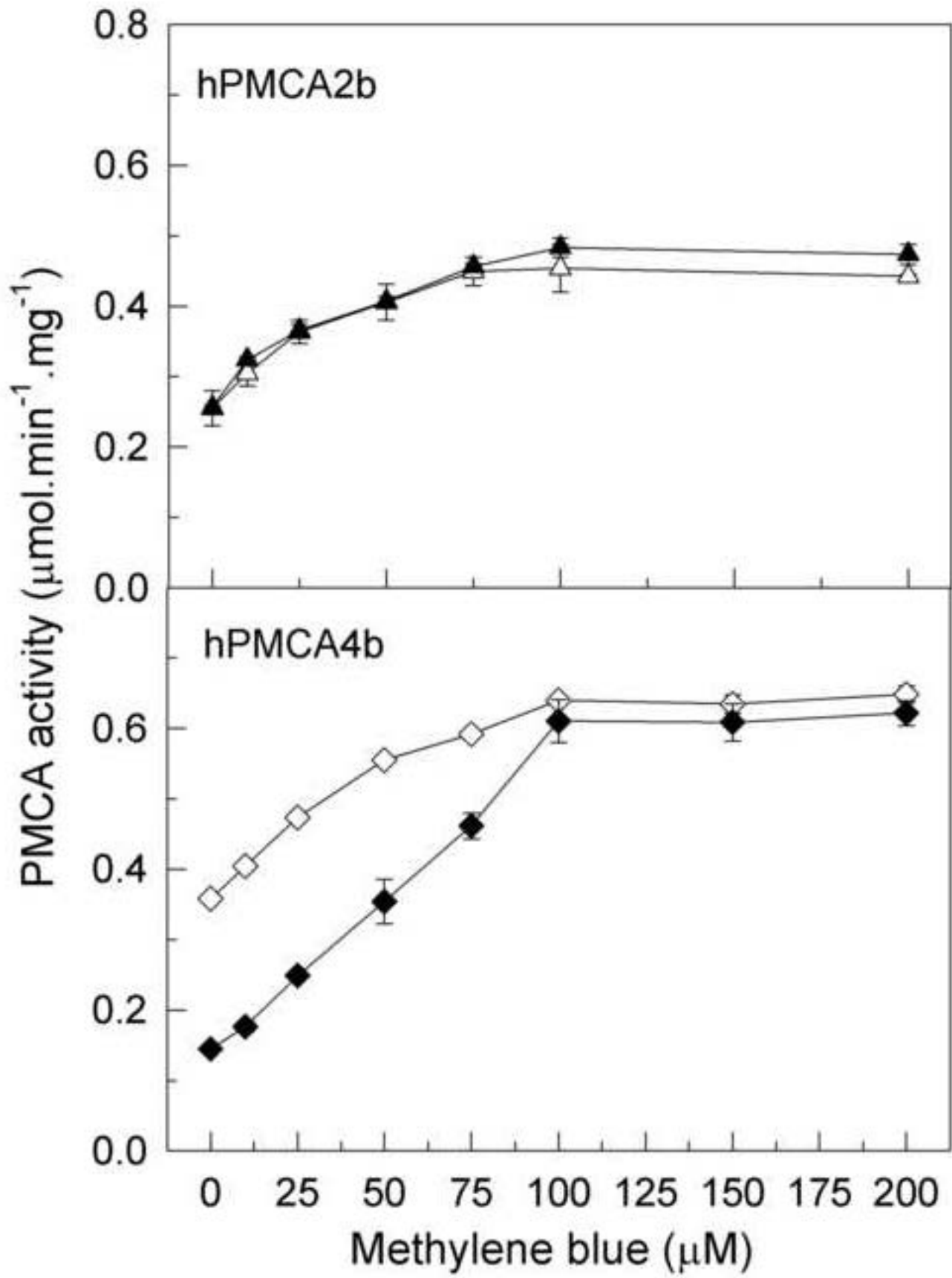


Figure 4
[Click here to download high resolution image](#)

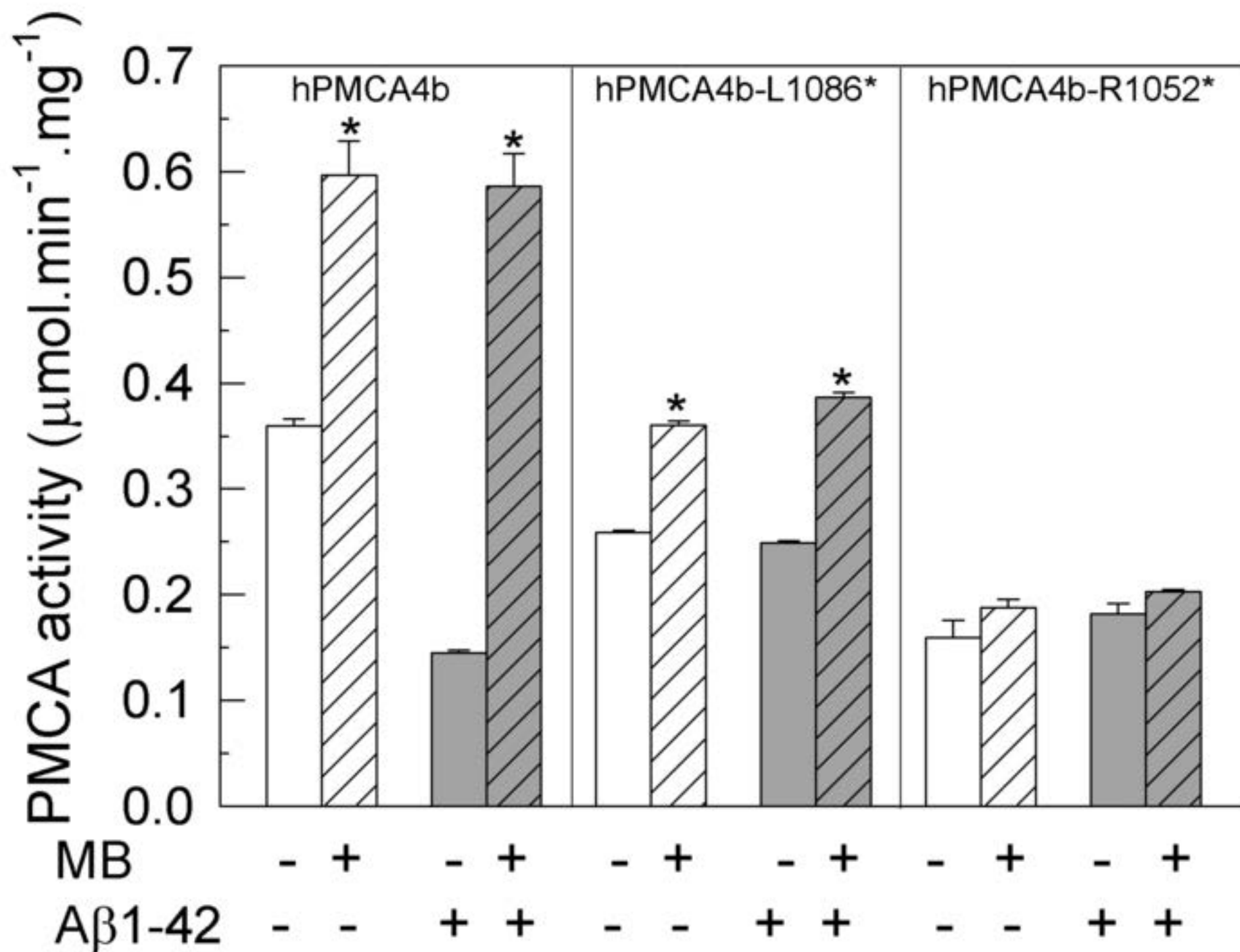


Figure 5
[Click here to download high resolution image](#)

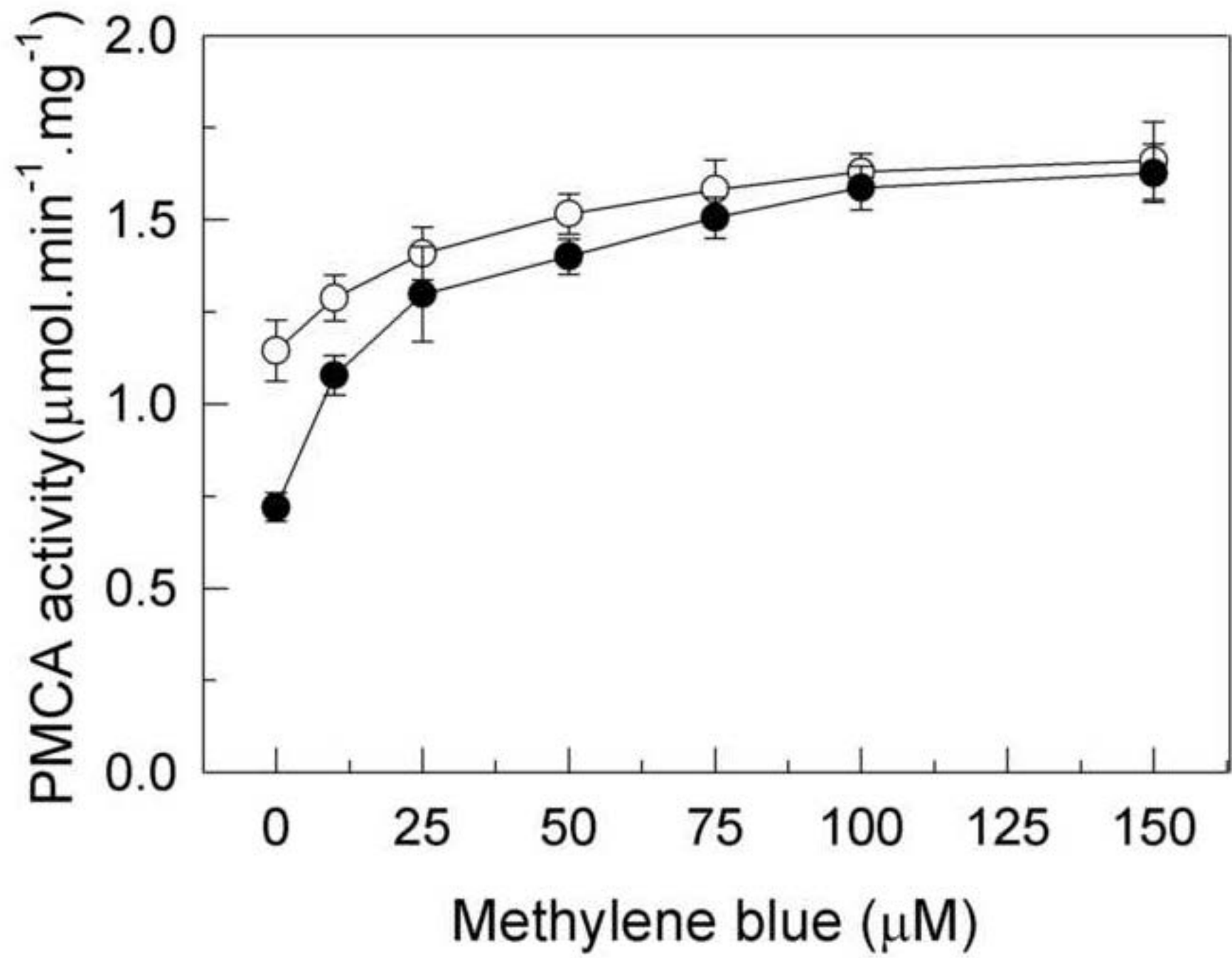


Figure 6

[Click here to download high resolution image](#)

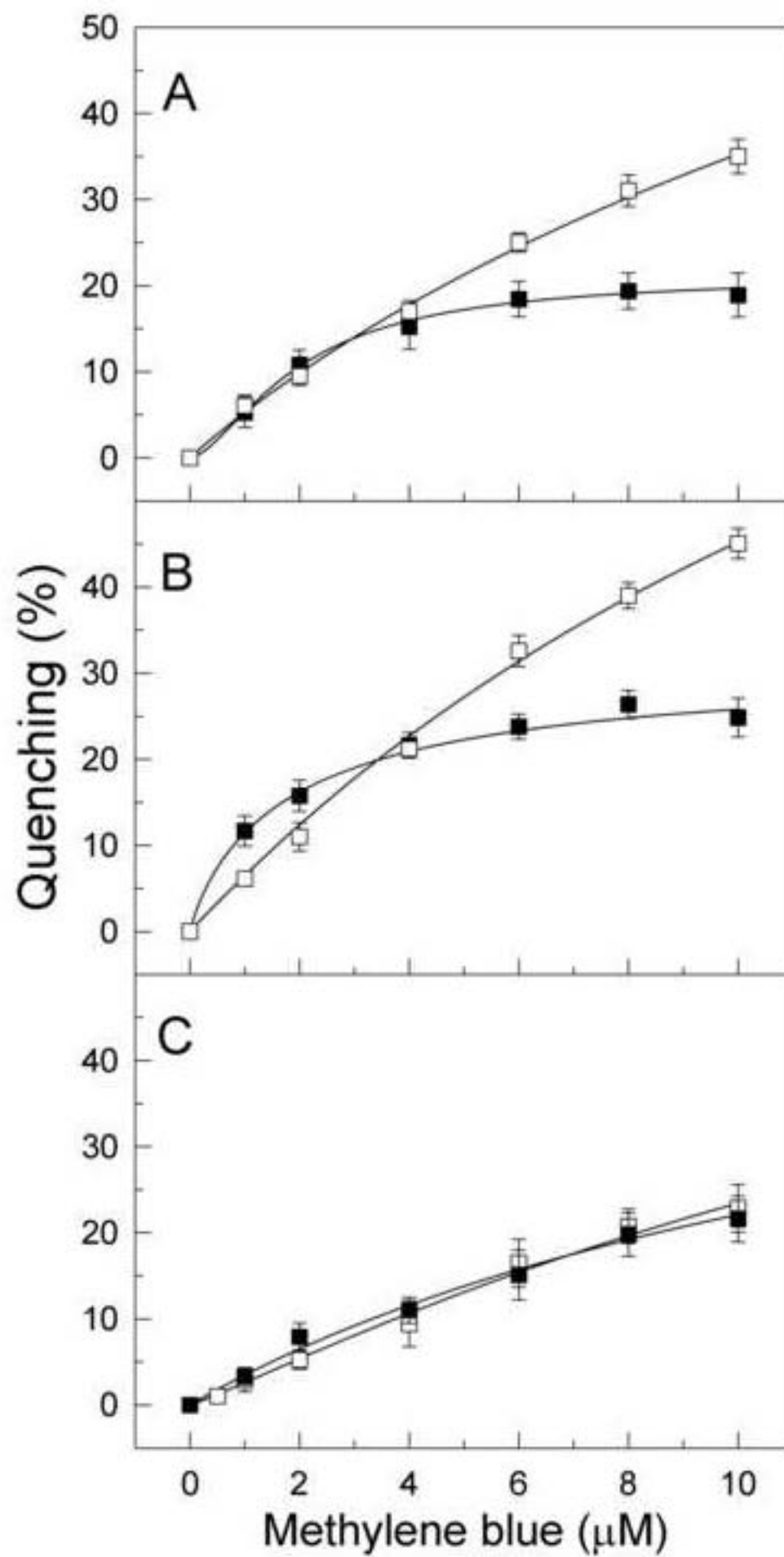


Figure 7
[Click here to download high resolution image](#)

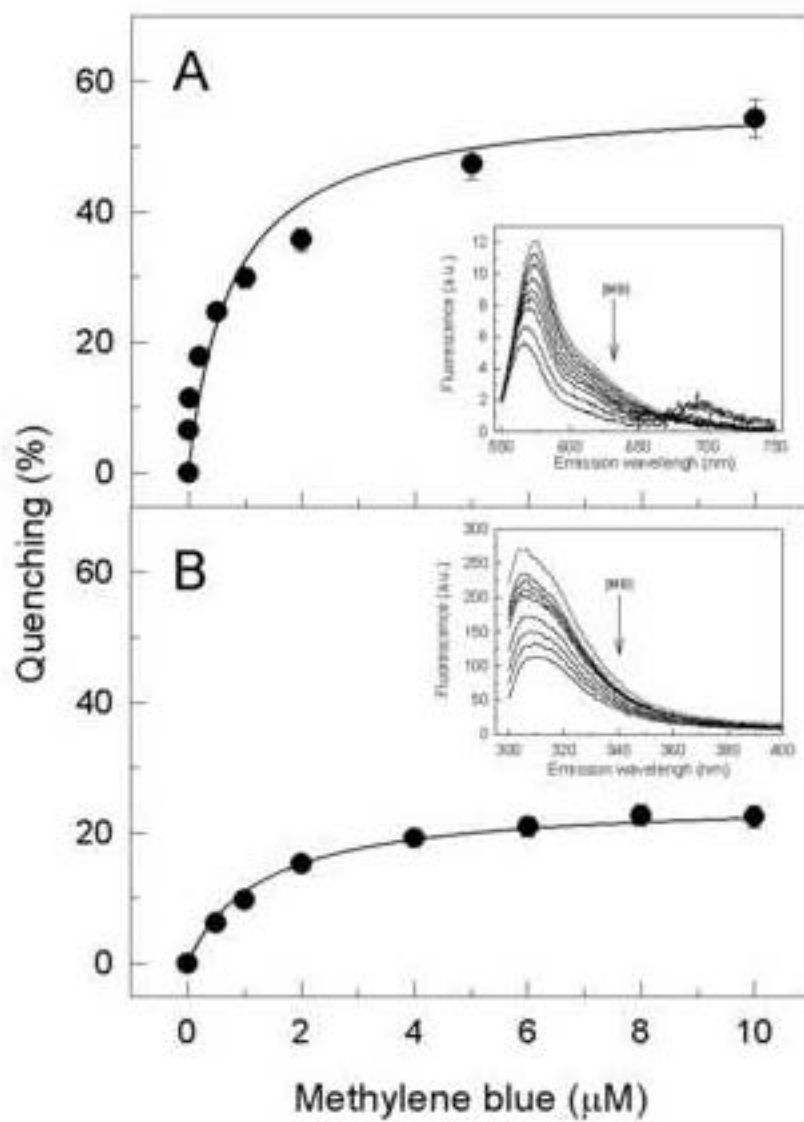
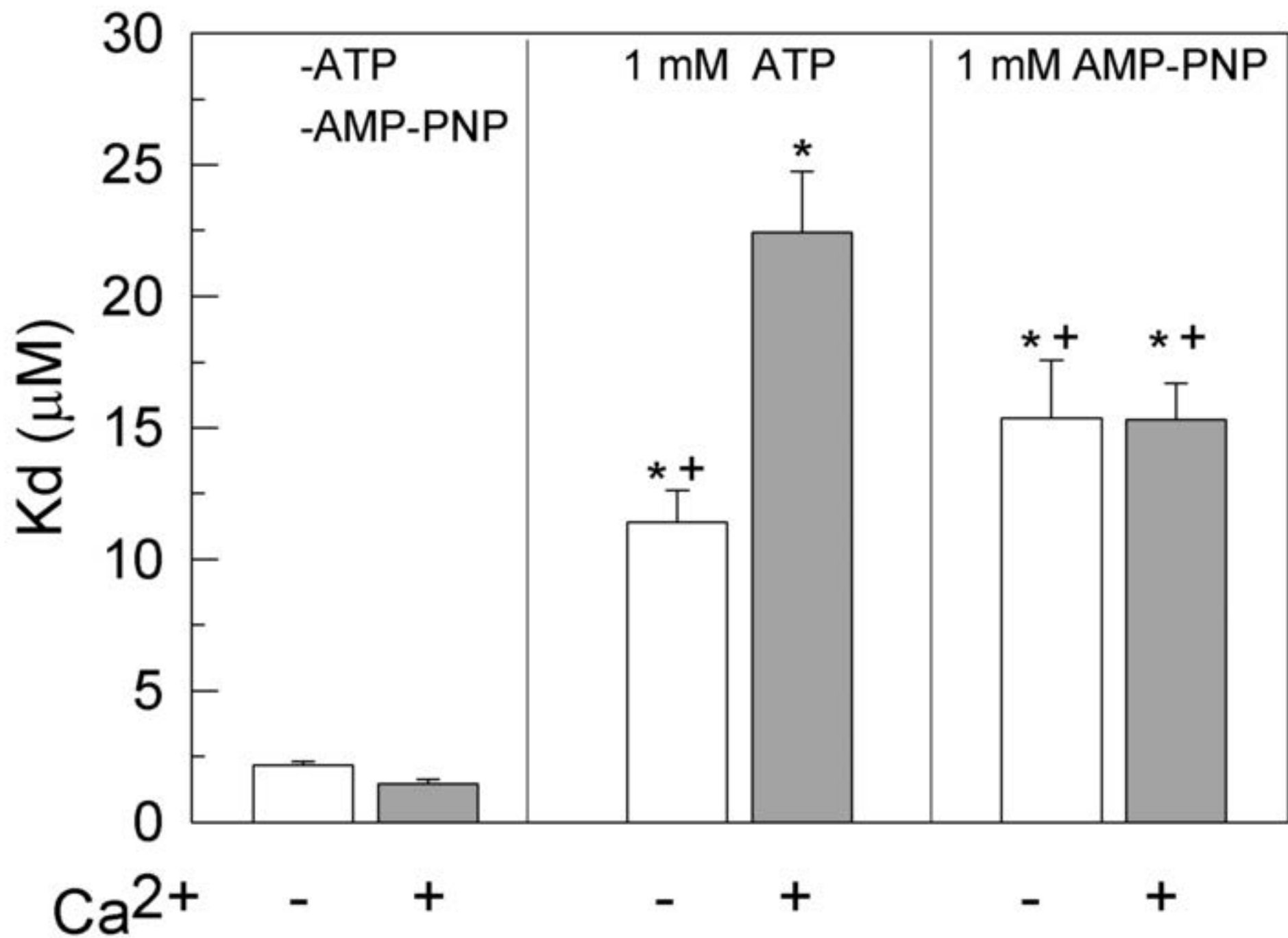


Figure 8
[Click here to download high resolution image](#)



Supplemental fig. Full WB of Figure 2

[Click here to download Supplementary Material: FullWB-PMCAisoforms .tif](#)